

Supersolid phase in atomic gases with magnetic dipole interaction

Adam Bühler and Hans Peter Büchler

Institute for Theoretical Physics III, University of Stuttgart, Germany

(Dated: May 10, 2022)

A major obstacle for the experimental realization of a supersolid phase with cold atomic gases in an optical lattice is the weakness of the nearest-neighbor interactions achievable via magnetic dipole-dipole interactions. In this letter, we show that using a large filling of atoms within each well the characteristic energy scales are strongly enhanced. Within this regime, the system is well described by the rotor model, and the qualitative behavior of the phase diagram derives from mean-field theory. We find a stable supersolid phase for realistic parameters with chromium atoms.

PACS numbers: 03.75.Lm, 67.80.kb, 67.85.Hj

Magnetic dipole-dipole interactions offer a remarkable opportunity to explore quantum phenomena with long range interactions in cold atomic gases. Of special interest are atoms with large magnetic dipole moments such as Cr, where the influence of the dipole-dipole interactions on the atomic cloud as well as the dipole induced collapse have been observed [1–3]. In the presence of an optical lattice, the system gives naturally rise to extended Hubbard models with nearest-neighbor interactions [4], and many remarkable quantum states have been predicted [5–8]. A major obstacle towards the experimental realization of these states is the weakness of the nearest-neighbor interaction due to the magnetic character of the dipole-dipole potential, and correspondingly the extremely stringent requirements on temperature, trapping potentials, and life-time of the atomic system. In this letter, we propose an experimentally realistic setup for the realization of a supersolid phase in cold atomic gases with magnetic dipole-dipole interactions.

A supersolid phase combines two seemingly contradiction properties, which in most materials appear in competition with each other: the arrangement of the particles in a crystalline structure with a superfluid transport of the particles [9]. While recent experimental observation of a superfluid response in solid ^4He are still controversial [10–12], various models in lattice systems have extensively been studied in the past and the existence of a supersolid phase has been demonstrated using quantum Monte Carlo simulations. Of special interest is the appearance of a supersolid phase in a triangular lattice [13] and the stabilization of a supersolid phase in a square lattice by dipole-dipole interaction [6]. These Hubbard models can be naturally realized with cold polar molecules or atomic gases with magnetic dipole-dipole interactions. While the understanding of the microscopic derivation of the Hubbard model for cold atomic gases is well understood [14], the nearest-neighbor interactions obtained for atoms in a characteristic optical lattice is well below a nano Kelvin, i.e., for Cr with strong magnetic dipole moment $V \approx 0.2\text{nK}$ with lattice spacing $a = 500\text{nm}$ – such stringent requirements have not yet been achieved in experiments.

In this letter, we demonstrate that the critical temperature for the supersolid phase can be increased by several orders of magnitude. This opens up a way towards the experimental realization of supersolids with cold atomic gases using the magnetic dipole-dipole interactions with current experimental technologies. The main idea is to allow a high filling factor of atoms per lattice site; then the influence of the dipole-dipole interaction is enhanced by the number of atoms within each well. In the extreme situation, the system is then described by a coupled array of Bose-Einstein condensates.

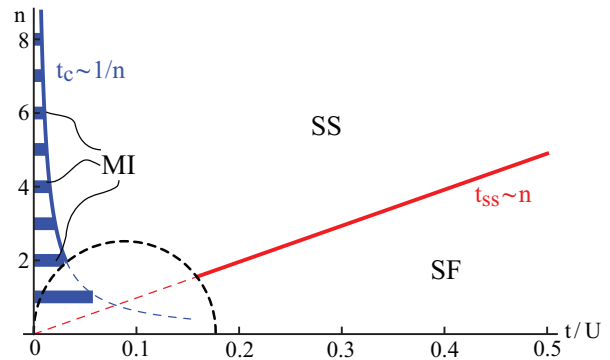


FIG. 1: Phase diagram for $U \sim V$: The Mott insulating/solid phases appear at commensurate fillings (solid bars) and the critical hopping at the tip of the incompressible lobes scales as $t_c \sim 1/n$. In turn, the transition from the superfluid into a supersolid phase behaves as $t_{ss} \sim n$, i.e., for large fillings $n \gg 1$ the influence of quantum fluctuations is reduced and the transition from the superfluid into the supersolid phase is well described within mean-field theory.

For low filling factors, the competition between the instability towards a supersolid phase and the Mott insulating phase for integer fillings gives rise to a rich phase diagram. Within this regime mean-field theory fails to correctly reproduce the phase diagram and it is mandatory to resolve to exact methods such as quantum Monte Carlo simulations [15]. On the other hand, for high filling factors the critical hopping t_c for the phase transition towards the solid phases/Mott insulators scales as $t_c \sim 1/n$, while the instability from the superfluid to

wards the supersolid phase appears at much higher hopping with $t_{ss} \sim n$, see Fig. 1. Consequently, the competition between the different phases is reduced and the phase diagram is well described within mean-field theory. In the following, we derive the transition towards the supersolid phase and find the optimal parameters for the experimental realization in cold atomic gases with magnetic dipole-dipole interactions.

We start with the description of the Hamiltonian for the cold atomic gases with magnetic dipole-dipole interactions. The system is confined into a quasi two-dimensional setup with an additional optical lattice within the plane. Each lattice site is occupied by many particles, and therefore, gives rise to a quasi-condensate on each lattice site. Note, that we assume a lattice spacing larger than the usual spacing in optical lattices in order to reduce losses from three-body recombinations. For such high filling factors, the validity of the standard Hubbard model breaks down. Nevertheless, the system exhibits tunneling between the different wells, and an interaction term accounting for deviations around the mean particle number n . Then, the Hamiltonian is well described by the rotor model

$$H = -2t \sum_{\langle ij \rangle} \sqrt{n_i n_j} \cos(\phi_i - \phi_j) + \frac{1}{2} \sum_{ij} V_{ij} \delta n_i \delta n_j, \quad (1)$$

where $\delta n_i = n_i - n$ describes the deviation from the mean particle density n within each well, while ϕ_i denotes the phase within each well satisfying the commutation relation $[n_i, \phi_j] = i\delta_{ij}$. The interaction term V_{ij} contains an on-site interaction U for $i = j$, and obeys the characteristic decay $V_{i \neq j} = Va^3/|\mathbf{R}_i - \mathbf{R}_j|^3$ for dipole-dipole interactions with a the lattice spacing and \mathbf{R}_i the lattice vectors. Note, that the rotor model derives from the Hubbard model in the limit of large filling factors, however, the rotor model remains a proper description of bosonic atoms in an optical lattice even in the regime where several higher bands are occupied. Its phase diagram has previously been studied close to half filling $n \sim 1/2$ [16, 17]. Here, we first derive the phase diagram of the rotor model at large filling $n \gg 1$, and present the effective parameters for a realistic experiment with chromium atoms in a second step.

The system is in the superfluid phase for dominant hopping with $t \gg V, U$, and is characterized by a fixed phase ϕ within each well and a homogeneous particle density n . Its mean-field energy per lattice site reduces to $E_0/N = (U + V\chi_0)n^2/2 - 2tnz$ with $z = 4$ the number of nearest-neighbors and N the number of lattice sites. Here, $\chi_{\mathbf{k}} = \sum_{j \neq 0} \exp(i\mathbf{k}\mathbf{R}_j)/|\mathbf{R}_j|^3$ denotes the dipole-dipole interaction in momentum space. The transition towards the supersolid phase for increasing interactions is signaled by an instability in the excitation spectrum. Expanding the Hamiltonian to second order in fluctuating fields $\delta n_i = n_i - n$ and $\delta \phi_i = \phi_i - \phi$ around the

mean-field values, and introducing the momentum representation with $\delta \phi_{\mathbf{k}} = \sum_j \exp(i\mathbf{k}\mathbf{R}_j) \delta \phi_j / \sqrt{N}$ and analog for $\delta n_{\mathbf{k}}$, we obtain the Hamiltonian H_{n} describing the excitation spectrum above the superfluid ground state

$$H_{\text{n}} = \sum_{\mathbf{k}} \left(\epsilon_{\mathbf{k}} \delta \phi_{\mathbf{k}} \delta \phi_{-\mathbf{k}} + \tilde{V}_{\mathbf{k}} \delta n_{\mathbf{k}} \delta n_{-\mathbf{k}} \right) = \sum_{\mathbf{k}} E_{\mathbf{k}} a_{\mathbf{k}}^{\dagger} a_{\mathbf{k}},$$

with the single particle dispersion relation $\epsilon_{\mathbf{k}} = 2tn[z - 2\sum_{\alpha} \cos(\mathbf{k}\mathbf{e}_{\alpha})]$ and the effective interaction $\tilde{V}_{\mathbf{k}} = \epsilon_{\mathbf{k}}/(2n)^2 + U(1 + \gamma\chi_{\mathbf{k}})/2$. Here, $\gamma = V/U$ denotes the ratio between the strength of the dipole-dipole interaction V and the on-site interaction U , whereas \mathbf{e}_{α} accounts for the unit vectors in direction of the nearest-neighbor lattice sites. Introducing the creation (annihilation) operators $a_{\mathbf{k}}^{\dagger}$ ($a_{\mathbf{k}}$) for the excitations above the superfluid ground state through $a_{\mathbf{k}}^{\dagger} = i\beta_{\mathbf{k}}\delta\phi_{\mathbf{k}} + \delta n_{-\mathbf{k}}/2\beta_{\mathbf{k}}$ with $\beta_{\mathbf{k}}^4 = \epsilon_{\mathbf{k}}/4\tilde{V}_{\mathbf{k}}$, we obtain the excitation spectrum of the superfluid phase $E_{\mathbf{k}} = (4\tilde{V}_{\mathbf{k}}\epsilon_{\mathbf{k}})^{1/2}$.

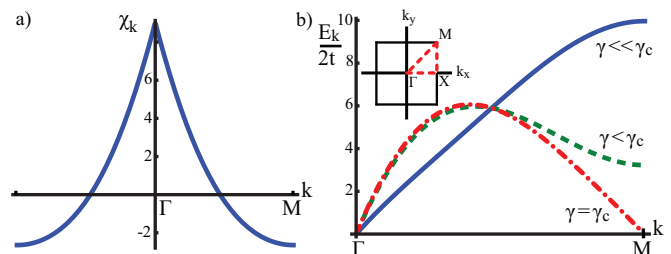


FIG. 2: **a)** Shape of the Fourier transformed dipole-dipole interaction $\chi_{\mathbf{k}}$ plotted in the M -direction. **b)** Superfluid dispersion relation for different values of γ . At $\gamma = \gamma_c$ the Roton minima occurs. The inset shows the different directions within the Brillouin zone.

Next, we analyze the stability of the superfluid phase by varying the ratio γ between the dipole strength and the on-site interaction. The result strongly depends on the lattice geometry. Here, we focus on a square lattice with lattice spacing a ; the generalization to arbitrary lattice structures is straightforward. The quantity $\chi_{\mathbf{k}}$ is maximal at zero momentum with $\chi_0 \approx 9.02771$, while it turns negative and minimal at the edge of the Brillouin zone with $\mathbf{K} = (\pi/a, \pi/a)$ and $\chi_{\mathbf{K}} \approx -2.64589$, see Fig. 2a. As a consequence, the excitation spectrum exhibits a Roton minima for increasing dipole-dipole interactions, see Fig. 2b, and eventually turns zero $E_{\mathbf{K}} = 0$ at the critical value

$$\gamma_c = \frac{1}{|\chi_{\mathbf{K}}|} \left(\frac{2zt}{Un} + 1 \right). \quad (2)$$

Hence, the superfluid phase suffers an instability at γ_c via the nucleation of excitations with momenta \mathbf{K} . In general, one expects that these excitations form a second condensate and give rise to a density modulation for the system. The novel ground state is characterized by a

superfluid response due to the condensates at $\mathbf{k} = 0$ and \mathbf{K} , and a solid order, i.e., the instability signals a phase transition from a superfluid into a supersolid.

Now, we analyze the stability and the ground state properties of the novel phase by a mean-field ansatz with two condensates. For this purpose, we introduce a density modulation $\bar{n}_j = |c + d \exp[i(\mathbf{K}\mathbf{R}_j + \theta)]|^2$ with the constraint $c^2 + d^2 = n$. The density modulation appears as the inference of the two condensates at $\mathbf{k} = 0$ and \mathbf{K} with the relative phase θ , and exhibits a checkerboard structure. Inserting this ansatz into the rotor Hamiltonian (1), we obtain the energy per lattice site

$$\frac{E_{ss}(d, \theta)}{N} = \frac{E_0}{N} + 4zt d^2 - 2d^2 (n - d^2) \cos^2 \theta (|\chi_{\mathbf{K}}| V - U). \quad (3)$$

Here, E_0 is again the mean-field energy of the superfluid phase. The second term accounts for an increase of kinetic energy due to a reduction of coherence between the different wells, while the last term describes the lowering of the interaction energy via the density modulation. The ground state is obtained by minimizing the energy with respect to the density modulation and the relative phase between the two phases. The optimization of the phase requires $\theta = 0, \pi$, which corresponds to the two degenerate ground states reflecting the broken (discrete) translational symmetry. In the following, this phase will be absorbed into the sign of d . On the other hand, the condensate fraction d for the mode \mathbf{K} exhibits the typical Ginzburg Landau behavior for a second order phase transition and predicts the lowering of the ground state energy for $\gamma > \gamma_c$, i.e., the appearance of the supersolid phase within mean-field theory coincides with the instability of the excitation spectrum. The gain in energy via the formation of the supersolid phase takes the form

$$\frac{E_{ss} - E_0}{N} = -\frac{n^2 V}{2} \frac{|\chi_{\mathbf{K}}|^2}{|\chi_{\mathbf{K}}| - 1/\gamma} \left(1 - \frac{\gamma_c}{\gamma}\right)^2. \quad (4)$$

A special property of the energy gain is, that it scales with the square of the number of particles per lattice site n . The supersolid phase is characterized by a checkerboard density modulation with the order parameter Δ defined by the correlation function

$$\langle \bar{n}_i \bar{n}_j \rangle = n^2 [1 + \Delta^2 \cos(\mathbf{K}(\mathbf{R}_i - \mathbf{R}_j))], \quad (5)$$

for $|i - j| \rightarrow \infty$ and a superfluid density n_s describing the superfluid flow. Within mean-field theory, these quantities reduce to $n_s = 2tz / (|\chi_{\mathbf{K}}| V - U)$, and $\Delta^2 = 1 - n_s^2 / n^2$. Note, that within a supersolid, the superfluid density is reduced compared to the averaged density, i.e., $n_s < n$ even at zero temperature due to the additional solid structure [9].

The most remarkable result in Eq. (4) is the scaling of the gain in energy via the formation of the supersolid phase with the number of particles in each lattice site,

i.e., $(E_{ss} - E_0)/N \sim n^2 V/2$. This energy serves as an estimate for the critical temperature T_{solid} for the formation of the solid structure, i.e., at optimal values the critical temperature $T_{\text{solid}} \sim n^2 V/2$ is strongly enhanced compared to the single particle nearest-neighbor energy V . This observation is in agreement with the recently predicted formation of solid structures in very large superlattices [18]. The detailed estimation of the energy scales for realistic experimental setup is shown below.

Finally, we check the stability of the supersolid phase against quantum fluctuations and determine the excitation spectrum above the supersolid ground state. Again we introduce the fluctuating field operators $\delta\phi_i = \phi_i - \phi$ and $\delta n_i = n_i - \bar{n}_i$, where $\bar{n}_i/n = 1 + \Delta \cos(\mathbf{K}\mathbf{R}_i)$ denotes the mean particle density per lattice site within the mean-field theory exhibiting a checkerboard structure. Then, the Hamiltonian expanded to second order in these operators reduces to

$$H_{ss} = tn_s \sum_{\langle i, j \rangle} \left[(\delta\phi_i - \delta\phi_j)^2 - \frac{\delta n_i \delta n_j}{2n_s^2} \right] + \frac{tz}{2n_s} \sum_i \delta n_i^2 \frac{1 + \Delta^2 - 2\Delta \cos(\mathbf{K}\mathbf{R}_i)}{1 - \Delta^2} + \frac{1}{2} \sum_{ij} V_{ij} \delta n_i \delta n_j. \quad (6)$$

Note, that the third term involves the modulated density with wave vector \mathbf{K} . As a consequence, this introduces a coupling for modes with momentum \mathbf{k} and $\mathbf{k} + \mathbf{K}$, which becomes obvious in the moment representation

$$H_{ss} = \sum_{\mathbf{k}} [\xi_{\mathbf{k}} \delta\phi_{\mathbf{k}} \delta\phi_{-\mathbf{k}} + \zeta_{\mathbf{k}} \delta n_{\mathbf{k}} \delta n_{-\mathbf{k}} + \eta \delta n_{\mathbf{k}} \delta n_{-(\mathbf{k}+\mathbf{K})}],$$

with the parameters $\xi_{\mathbf{k}} = 2tn_s[z - 2\sum_{\alpha} \cos(\mathbf{k}\mathbf{e}_{\alpha})]$,

$$\zeta_{\mathbf{k}} = \frac{U + \chi_{\mathbf{k}} V}{2} + \frac{zt}{2n_s} \left[\frac{1 + \Delta^2}{1 - \Delta^2} - \frac{2}{z} \sum_{\alpha} \cos(\mathbf{k}\mathbf{e}_{\alpha}) \right],$$

and $\eta n_s = -zt \Delta / (1 - \Delta^2)$. This coupling is a result of the broken translational symmetry in the supersolid phase, which reduces the Brillouin zone. Hence, we obtain two modes for each momentum value \mathbf{k} with the dispersion relation, see Fig. 3,

$$(E_{\mathbf{k}}^{\pm})^2 = 2(\xi_{\mathbf{k}} \zeta_{\mathbf{k}} + \xi_{\mathbf{k}+\mathbf{K}} \zeta_{\mathbf{k}+\mathbf{K}}) \pm 2\sqrt{(\xi_{\mathbf{k}} \zeta_{\mathbf{k}} - \xi_{\mathbf{k}+\mathbf{K}} \zeta_{\mathbf{k}+\mathbf{K}})^2 + 4\zeta_{\mathbf{k}} \xi_{\mathbf{k}+\mathbf{K}} \eta^2}. \quad (7)$$

The lower branch of the dispersion relation accounts for the acoustic modes with a linear sound mode for small values \mathbf{k} , while the second branch accounts for density fluctuations of the checkerboard order. Due to the discrete translational symmetry this mode is lifted to a finite value for small values \mathbf{k} and corresponds to an optical mode. From the dispersion relation Eq. (7), we find that the supersolid phase is stable.

Finally, we can estimate the relevant parameters for the experimental realization of a supersolid phase for

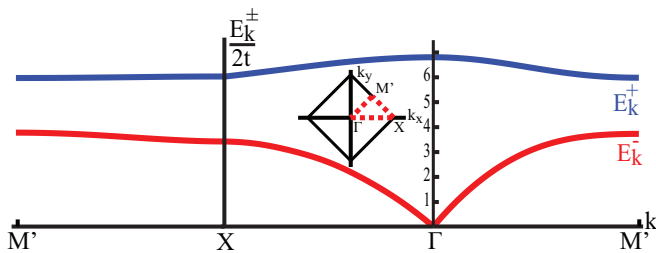


FIG. 3: Supersolid dispersion relation, given in different directions of the reduced Brillouin zone, as shown in the inset.

chromium atoms in an optical lattice [19]. The limiting energy is given by the nearest-neighbor interaction V for magnetic dipole-dipole interactions. These interactions are characterized by the length scale $a_{dd} = \mu_0 \mu^2 m / (12\pi \hbar^2) \approx 0.8 \text{ nm}$, where μ is the permanent magnetic dipole moment. Then, the strength V of the dipole-dipole interaction reduces to

$$V = \frac{6}{\pi^2} \frac{a_{dd}}{a} E_r, \quad (8)$$

with $E_r = \pi^2 \hbar^2 / 2ma^2$ the recoil energy and a the lattice spacing. Starting with a conventional density for a BEC of cold atomic gases, we obtain a filling with $n \sim 40$ for a lattice spacing of $a \sim 1 \mu\text{m}$ within the plane and a prolate shape of each well along the perpendicular direction with aspect ratio $\lambda \approx 1/4$. The nearest-neighbor energy reduces to $V \approx 0.5 \text{ Hz}$, while the characteristic temperature scale for the formation of the solid structure reaches $T_{\text{solid}} \sim n^2 V / 2 \approx 0.4 E_r$. On the other hand, the on-site interaction within each well derives as the change of energy for the local condensate within the well by adding/removing particles, i.e., $U = \partial_n^2 E_{\text{local}}[n]$. Tuning the s-wave scattering length a_s across the Feshbach resonance present for chromium allows us to compensate the contribution from the dipole-dipole interaction, and consequently the on-site interaction can be tuned to an arbitrary small value. For particle numbers with $n \sim 40$ within the quasi-condensate, the influence of the interactions is weak on the ground state wave function, which is dominated by the contribution from the trap and kinetic energy. Then, the ground state wave function is well described by a Gaussian wave function and the on-site interaction reduces to (see Ref. [19] for details)

$$U = \frac{2\hbar\bar{\omega}a_{dd}}{\sqrt{2\pi}a_{ho}} \left[\frac{a_s}{a_{dd}} - f(\sqrt{\lambda}) \right], \quad (9)$$

where $\bar{\omega}$ is the mean trap frequency and a_{ho} the corresponding harmonic oscillator length, while $f(\sqrt{\lambda})$ denotes a dimensionless function with $f(1/2) \approx 0.5$. The result is derived within first order perturbation theory in the small parameter $a_{dd}n/a_{ho}$. The stability against collapse of the quasi-condensate is well guaranteed for such small particle numbers.

The last remaining parameter is the tunneling energy t . From the critical value γ_c in Eq. (2), we find that the tunneling has to be suppressed by the factor $t < Vn|\chi_{\mathbf{K}}|/8 \approx 6.2 \text{ Hz}$. Note, that the allowed energies for the hopping term increases again with the number of particles. In addition, the superfluid stiffness involves another factor n . As a consequence, the appearance of the superfluid response given by the Kosterlitz-Thouless temperature $T_{\text{KT}} \sim \hbar^2 n_s / m$ exhibits the same scaling as the transition temperature for the solid, i.e., $T_{\text{KT}} \sim n^2 V / 2$. It is this scaling of the critical temperatures for the solid critical temperature as well as the Kosterlitz-Thouless temperature, which allows us to improve the experimental parameters by increasing the particle numbers within each well. The suitable experiments then can be performed by adiabatically ramping up the optical lattice in a BEC of chromium atoms at positive s-wave scattering length a_s until the proper filling and hopping energies are reached. Within this method, temperatures well below the recoil energy can be reached [20]. Then, lowering the s-wave scattering length allows one to pass through the supersolid instability and the additional formation of the solid structure.

Discussions with T. Pfau are acknowledged. The work was supported by the Deutsche Forschungsgemeinschaft (DFG) within SFB/TRR 21.

-
- [1] A. Griesmaier, et al., Phys. Rev. Lett. **94**, 160401 (2005).
 - [2] T. Koch et al., Nat Phys **4**, 218 (2008).
 - [3] Q. Beaufils et al., Phys. Rev. A **77**, 061601 (2008).
 - [4] K. Góral, L. Santos, and M. Lewenstein, Phys. Rev. Lett. **88**, 170406 (2002).
 - [5] P. Sengupta, et al., Phys. Rev. Lett. **94**, 207202 (2005).
 - [6] B. Capogrosso-Sansone, et al., Phys. Rev. Lett. **104**, 125301 (2010).
 - [7] L. Pollet, et al., Phys. Rev. Lett. **104**, 125302 (2010).
 - [8] I. Danshita and C. A. R. Sá de Melo, Phys. Rev. Lett. **103**, 225301 (2009).
 - [9] A. J. Leggett, Phys. Rev. Lett. **25**, 1543 (1970).
 - [10] E. Kim and M. H. W. Chan, Nature **427**, 225 (2004).
 - [11] J. D. Reppy, Phys. Rev. Lett. **104**, 255301 (2010).
 - [12] B. K. Clark and D. M. Ceperley, Phys. Rev. Lett. **96**, 105302 (2006).
 - [13] S. Wessel and M. Troyer, Phys. Rev. Lett. **95**, 127205 (2005); D. Heidarian and K. Damle, Phys. Rev. Lett. **95**, 127206 (2005); R. G. Melko et al., Phys. Rev. Lett. **95**, 127207 (2005).
 - [14] D. Jaksch, et al., Phys. Rev. Lett. **81**, 3108 (1998).
 - [15] F. Hébert et al., Phys. Rev. B **65**, 014513 (2001).
 - [16] A. van Otterlo and K.-H. Wagenblast, Phys. Rev. Lett. **72**, 3598 (1994).
 - [17] E. Roddick and D. Stroud, Phys. Rev. B **51**, 8672 (1995).
 - [18] T. Lahaye, T. Pfau, and L. Santos, Phys. Rev. Lett. **104**, 170404 (2010).
 - [19] T. Lahaye, et al., Rep. Prog. Phys. **72**, 126401 (2009).
 - [20] I. Bloch, J. Dalibard, and W. Zwerger, Rev. Mod. Phys. **80**, 885 (2008).